A Review: Graphene Photonic Crystal Fiber

Zainab Mohammed AL-Wahhamy[1], Muwafaq F. Jaddoa[1] and

Firas Faeq K. Hussain[1,2,*]

[1]*Department of Physics, College of Science, Al-Muthanna University , Muthanna, Iraq*

[2]*College of Engineering, Al-Ayen Iraqi University, Dhi-Qar, Iraq*

[*]*Corresponding author: muwafaq_fj@mu.edu.iq*

Received 22 Apr, 2024, Accepted 1 June. 2024, published 1 Jun 2024.

DOI: 10.52113/2/11.01.2024/62-93

Abstract: Next-generation optical fibers with diverse operating mechanisms, high functionality, and a porous structure that may be designed are known as photonic crystal fibers, or PCFs. In the meantime, two-dimensional graphene, possessing incredibly unique characteristics, is a perfect material for optoelectronic and optical uses. Recently, many studies have been published based on the integration of graphene with PCFs to create a new graphene PCF (Gr-PCF). There hybrid fibers show outstanding light-mater interaction over a broad spectrum range. This review starts with general introduction about photonic crystal fiber and analysis of optical properties. This is followed by a Plasmonic PCF then Graphene and physico-chemical properties of graphene nanomaterials. The review primarily covers the introduction of graphene and PCFs with many Applications including Optics Communications and different physical sensors.

Keywords: photonic crystal fiber, Graphene, fiber laser devices, sensors, surface plasmon resonance (SPR).

1. Introduction

Photonic Crystal Fibers (PCFs) are a unique type of optical fiber with a range of applications for light guiding and modification. They are also sometimes referred to as microstructured or holey fibers. Because of a periodic arrangement of air holes arranged down their length, PCFs are constructed differently from regular optical fibers in that they have a lattice of photonic crystals inside the fiber core [1,2].

The development of PCFs allowed for exact control over the properties of light propagation, which completely changed the field of fiber optics. Similar to the bandgap in electrical materials, the periodic arrangement of air holes in PCFs produces a bandgap that permits light to be guided through a photonic band structure. This bandgap, sometimes referred to as the photonic stopband, allows PCFs to be highly customized for a variety of applications by being able to be adjusted to particular wavelengths or frequency ranges[3].

PCFs are used to confine light in a solid or hollow core region, depending on the

design, is one of their main advantages. Numerous applications, including high-power delivery, nonlinear optics, supercontinuum production, and sensing, are made possible by this special characteristic [4,5]

PCFs are superior than conventional optical fibers in a number of ways. Control over dispersion, nonlinear effects, and confinement qualities are made possible by their special structural design, which may be tailored for certain uses. Additionally, PCFs make it possible to integrate other elements into the fiber structure, creating opportunities for improved performance and functionalization [6].

PCFs have been used in many different industries throughout the years, including biomedical imaging, sensing, fiber lasers, high-power laser delivery, and telecommunications. Constant research and development in PCF technology keeps pushing the envelope of what's feasible in fiber-optic systems and light manipulation [7,8].

2. Photonic Crystal

It is crucial to understand photonic crystals and related photonic bandgap phenomena because PCFs use a 2-D photonic crystal structure for light steering. Periodic fluctuations in the dielectric constant within the order of the operating wavelengths generate photonic crystals. Compared to TIR in traditional optical fiber waveguides, photonic crystals are able to guide light far more efficiently. The concept of electronic bandgap in materials is a well. Electronics and photonics play equally significant roles in the concept of bandgaps, which refer to regions or energy levels within a material where electrons or photons cannot exist. In certain frequency bands or wavelengths, light waves may be prohibited from propagating, creating what is known as a photonic bandgap. By carefully selecting the crystal structure, adjusting the periodic lattice dimensions, and considering the properties of the constituent materials, it is possible to create and control these bandgaps within the crystal . Incoming light interacting with photonic crystal structure (which serves as a cladding in PCFs) would be totally internally reflected at some wavelengths even with a lower refractive index air core, resulting in guidance of those particular wavelengths. When

photonic crystal structures are put to fibers, PCFs are created [15].

3. Types of PCF

A photonic crystal fiber (PCF) is a structure made up of a core and cladding layers that follows the same propagation law of TIR as a regular fiber. Periodic nanostructures affect photon mobility in the same way that this ionic lattice affects electrons in materials [7]. The core of PCF is made of silica, which can be solid or hollow. The fiber's "holey" or "micro structured" look comes from the air holes surrounding the core. These holes enable light to be directed and passed through the core [9]. Different structures tend to imply that it is constituted of two types:

• Index guiding photonic crystal fiber

• Photonic band gap fiber.

3.1 Index guiding photonic crystal fiber

The PCF light is centered in the index guided by the complete internal reflection between the solid core and various air gap claddings. Air gap management on a micron scale is achieved by enveloping the solid core of the PCF file with a 1.462 refractive index pure silica cladding. Since the refractive indices of silica (1.462) and air (1.000) are so dissimilar, the light is centred by total internal reflection, which is one wavelength. The Effective Refractive Index is mainly used to measure the stage delay per unit length in PCF as compared to stage delay in vacuum.

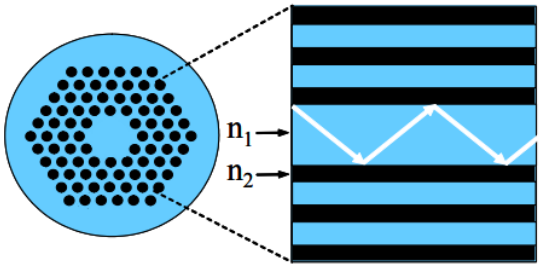

Fig. (1): Index-guidance, n1=1.45 (silica) and n2=1 (air).[10]

3.2 Photonic Band-gap Fiber

When the central portion of the air hole array is replaced with a hole that is considerably larger in diameter than the surrounding holes, a structure known as a photonic band-gap fiber is produced. The periodic fractured structure deforms and modifies its optical characteristics. Therefore, the electromagnetic modes impossibly reproduced in the holes. Its impact can be observed in photonic crystal band-gap fibers, where the low index core region's light is regulated by the wavelength. The frequency of the outside light determines how well the

fiber can confine light. Light is guided through the holes in the fiber and eventually confined if this recurrence occurs at the same time as the band-gap recurrence. Consequently, a large center refractive index is not required [11].

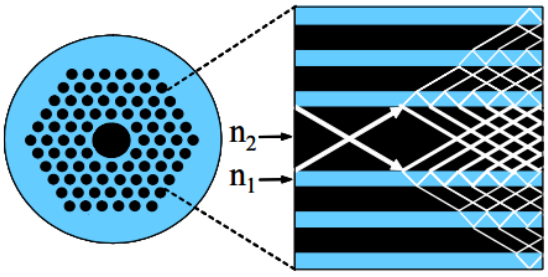

Fig. (2): Bandgap-guidance, n1=1.45 (silica) and n2=1 (air).[10]

4. Analysis of optical properties

The paper discusses the key features of PCF such as birefringence, nonlinearity, chromatic dispersion, confinement loss, effective mode area, and zero dispersion wavelengths.

4.1 Birefringence

Birefringence is a crucial property required in various detection devices and fiber optics, where maintaining a well-defined polarization of light is important. Birefringence arises from the lack of symmetry in the optical properties of certain materials, often referred to as the optical pivot or center of symmetry. This phenomenon is commonly observed in materials that exhibit uniaxial anisotropy [12]. In the presence of birefringence, linearly polarized light beams traveling in parallel and opposite directions experience unequal effective refractive indices, denoted as n_e and n_0 , respectively. As a result, the oppositely polarized segment of light may undergo refraction at a standard angle according to the law of refraction, while the other segment deviates from the standard angle due to the difference in the refractive indices. This difference in refractive indices, known as the birefringence magnitude, leads to non-standard refraction behavior when unpolarized light passes through a material with a non-zero birefringence angle with respect to the optical pivot [13].

$$\Delta n = n_e - n_0 \qquad (1)$$

The variation in the real part values of the observable core own modes' effective indices and the x- and y-axes (LP01x and LP01y).

$$B = \left|Re\left(n_{xeff}\right) - Re\left(n_{xeff}\right)\right| \qquad (2)$$

4.2 Chromatic Dispersion

The chromatic dispersion or total dispersion is increased when the waveguide and material dispersions are combined. All-out scattering is subject to

change, but waveguide dispersion can only be altered by modifying the waveguide's plan parameter. The use of material to make the fiber is the only use of the material dispersion. The material dispersion can be ignored when nm (λ) stabilizes and the true portion of the effective index of refraction (n_{eff}) incorporates the scattering data [13].

$$D(\lambda) = -\frac{\lambda}{c}\frac{d^2 Re[n_{yeff}]}{d\lambda^2} \qquad (3)$$

Where D is the chromatic dispersion, λ is the operational wavelength, c is the speed of light in a vacuum and neff is the effective index of refraction of the PCF

4.3 Confinement Loss

Confinement Loss will inevitably happen when the optical mode leaks from the inner core region to the outer air holes due to the minimal number of air holes in the center region. Contention loss is computed from the imaginary component of the complex effective index neff using the fundamental mode approach.

$$L_c = \frac{40\pi}{ln\ ln\ (10)\lambda} Im(n_{eff}) \qquad (4)$$

The quantity of light that moves from the core material to the exterior matrix material is known as confinement loss. Pitch, air hole diameter, number of layers, and air hole count are all modifiable variables [13].

4.4 Effective Mode Area

The significance of the effective mode area lies in the fact that it influences the optical intensities within the fiber for a given power level. The smaller the effective mode area, the higher the optical intensities can be achieved. This emphasizes the importance of nonlinear effects in PCF, as the confined mode and small effective mode area enable higher optical power densities within the fiber. The following formulae yield the PCF's effective mode area, or A_{eff}:

$$A_{eff} = \frac{\left(\iint |E|^2 dxdy\right)^2}{\iint |E|^4 dxdy} \qquad (5)$$

E is the amplitude of the electric field. Even if the integration crosses the center zone, it still covers the whole plane. The significance of nonlinearities is highlighted by the tiny effective mode area that results in high optical intensities for a given power level [14].

4.5 Non-linearity

The non-linear coefficient of PCF is a crucial parameter in SCG analysis. SCG stands for Supercontinuum Generation. It

is a nonlinear optical phenomenon in which a broadband spectrum of light is generated by propagating intense laser pulses through a suitable medium. The nonlinear coefficient (γ) has an inverse relationship with the nonlinear refractive index (n_2) and is directly proportional to the effective area (A_{eff}) [14]. The nonlinear coefficient of PCF is given in eq. (6) :

$$\gamma = \frac{2\pi n_2}{\lambda A_{eff}} \qquad (6)$$

4.6 Zero Dispersion Wavelengths (ZDW)

ZDW, Zero Dispersion Wavelengths (ZDW), also known as second-order dispersion, refer to the points in the spectrum of optical fibers where the group delay dispersion becomes zero. In the case of photonic crystal fibers (PCFs) with small mode areas, they can exhibit wide waveguide dispersion, allowing for the adjustment of ZDW into the visible range. This leads to anomalous dispersion occurring in the visible wavelength range, enabling soliton transmission. PCFs and certain other fiber designs have the capability to generate three or more distinct ZDWs. When the pump light's wavelength is close to the ZDW, supercontinuum generation (SCG) can be used to generate extremely broad optical spectra. To summarize, ZDWs represent the wavelengths in optical fibers where the group delay dispersion becomes zero. In PCFs, the small mode areas and wide waveguide dispersion can enable the adjustment of ZDWs into the visible range, allowing for anomalous dispersion and soliton transmission. PCFs and other fiber designs can produce multiple ZDWs, and when the pump light's wavelength is near a ZDW, SCG can generate broad optical spectra [15].

5. Plasmonic in PCF

The capacity of these fibers to function as a substrate for the hosting of innovative functional optical materials within their air holes is one of their most significant characteristics. Examples include plasmonic material, gases, and liquids.Due of their strong interplay with visible light wavelengths, plasmonic metals like gold and silver are widely used. However, other materials, such as dielectrics or semiconductors (like graphene), can also exhibit plasmon-like activity at various frequency ranges.[16] Plasmonics has sparked optimism and sparked fresh ideas for device concepts by offering the ability to confine light at scales below the diffraction limit, a

capability that dielectric waveguides lack. Plasmonic devices find widespread use in various applications, such as power dividers, frequency splitters, and sensors. Plasmons, which are collective oscillations in electron gas density, are produced across a metal–dielectric interface or in bulk materials such as semiconductors and metals. The plasmon at the metal-dielectric interface is known as surface plasmon, or SP for short. It transforms into a surface plasmon polariton (SPP) when connected to electromagnetic waves that are applied externally [17].

6. Surface Plasmon Resonance (SPR)

When the electromagnetic field of a metal surface restricts and causes the collective oscillation of free electrons, surface plasmons (SPs) are produced [18]. A surface plasmon wave (SPW) travels in the transverse magnetic (TM) direction on a metal surface. Since the TE-polarization of the field component is perpendicular to the incident plane and cannot produce charge at the planar interface, a specific kind of TM-polarized light was selected to excite the SPs in plasmonics. When the interface that TM-polarized light travels along affects incident light, SP is created. The refractive index of the analyte will determine by changing the resonance location during sensing. When photons in a semiconductor or at a metal surface come into contact with electric dipoles, polaritons are excited. Surface plasmon polaritons (SPPs) are the polaritons that surface plasmons couple with [19]. The propagation of SPPs is directed at the interface between two different locations where metal and dielectric are present, as shown in Fig. 3. The resonance state that generates plasmonic waves at the metal-dielectric contact is known as surface plasmon resonance, or SPR. The fusion of photonics and plasmonics has led to the growth of coating technology, which in turn has aided in the creation of photonic sensors, which have garnered significant interest recently from the photonic community due to their potential applications. The PCF devices based on SPR coating with plasmonic materials offered extreme sensitivity [20].

One needs to meet the following requirement at the resonance. By satisfying this condition, constructive interference and resonant interactions can be achieved between the incident

light and the interface, leading to enhanced optical effects or phenomena.

$$\frac{2\pi}{\lambda} n_1 \, sin \, sin \, \theta = \frac{2\pi}{\lambda} \sqrt{\frac{\varepsilon_r n_2^2}{\varepsilon_r + n_2^2}} \qquad (7)$$

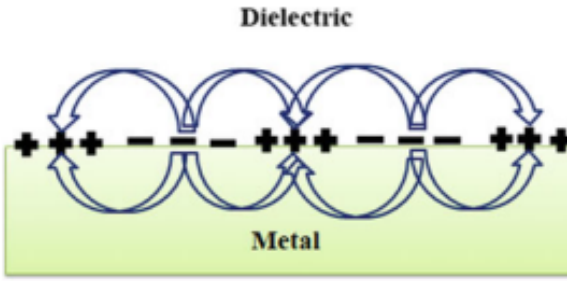

Fig. (3): Plasmonic generation at the metal-dielectric interface[18].

The plasmonic wave profile achieves its maximum and starts to rapidly diminish at the metal–dielectric interaction. The left and right sides of the expression (7) represent the wave vectors of the evanescent wave and the surface plasmon wave, respectively. Equation (7) indicates that the resonance peak is highly sensitive to variations in the refractive index, incident angle, and incident light wavelength of the analyte [20].

7. Graphene

The miracle Composites can be made from carbon material, a two-dimensional, single-atom-wide nanostructure with a large variable surface area. Because of its distinct physico-chemical properties and potential uses in energy storage devices, fuel cells, bioengineering, sensors, and analysis, among other fields, research teams have been captivated by graphene-based nanostructure. It is anticipated that graphene nanoparticles will revolutionize numerous other fields with a range of uses, such as electronics, optics, thermodynamics, and mechanics. During hybridization, these nanomaterials are frequently chemically treated to introduce functional groups through oxidation, doping with foreign atoms, and material reduction. A variety of techniques, such as "top down" and "bottom up," have been employed to produce graphene nanomaterials; each has advantages and disadvantages of its own [21,22].

8. Physico-Chemical Properties of Graphene Nanomaterials

The existence of a two-dimensional material was proven in 2004 with the isolation of monolayer graphene. High-resolution transmission electron microscopy (TEM) was then used to analyze the material and found that even little ripples can alter the layer arrangement in graphene. However, recent research indicates that the

incredibly robust and tenacious carbon-to-carbon bonds preserve graphene's stability [23].

8.1 Electronic Properties

A highly conductive substance, graphene is capable of carrying both electrons and holes as charge carriers. Because there is just one free electron for conduction out of the four valence electrons, it possesses special electrical properties [24].

The movable "pi" electrons, which occupy positions above and below the graphene layer, enhance the carbon-carbon bonds. The valence and conduction bands of graphene are connected to the bonding and anti-bonding of these "pi" orbitals.Graphene is a special material because its electrons and holes have zero effective mass at the Dirac points. The electrons and holes in the graphene Brillouin zone are called Dirac fermions, and there are six Dirac points in the zone. Nevertheless, there is minimal electric conduction at the Dirac points due to the absence of density states [25].

Graphene exhibits extraordinarily high electron mobility, with values up to around 15,000 cm2 V−1 s−1 and probably even higher. Electrons in graphene behave like photons when they move, and they can travel in a ballistic manner, meaning that they can go down sub-micrometer paths without scattering. The properties of graphene can be influenced by both its substrate and its own properties. On a silicon dioxide substrate, for example, graphene has a mobility of roughly 40,000 cm2 V−1 s-1 [26].

8.2 Mechanical Strength

Graphene is the strongest substance yet discovered due to its remarkable mechanical strength, which includes an ultimate tensile strength of 130 GPa [27]. Graphene weighs just 0.77 mg/m2, making it remarkably light in spite of its strength. At less than one gram in weight, a single layer of graphene—which is only one atom thick—can cover an entire football field. Elasticity is one of graphene's special qualities. It can withstand tension while still keeping its size and form. According to an atomic force microscope study of suspended graphene layers carried out in 2007, thicknesses ranging from 2 to 8 nm displayed spring constants in the range of 1–5 N/m and a Young’s modulus of 0.5 TPa, in contrast to three-dimensional graphite [28]. Originally, these

remarkable mechanical capabilities were based on theoretical predictions that assumed perfect, defect-free graphene. However, it has proven expensive and difficult to synthesize such perfect graphene. However, in an effort to cut expenses and get around these challenges, manufacturing techniques are progressively getting better [29].

8.3 Optical Properties Graphene

Graphene is only one atom thick, but it has peculiar visual characteristics. At 2.3%, it can absorb white light. The fine structural constant, which is unaffected by the material, controls the amount of light absorbed. About 2.3% of the light is absorbed by an additional layer of graphene. Graphene has an opacity of about 2.3% ($\pi\alpha \approx 2.3\%$) and a universal dynamic conductivity value of G = e2/4h (± 2-3%) throughout a range of observable frequencies [30].

Other characteristics of graphene include:

• Exceptional strength; although being lightweight, it is 200 times stronger than steel.

• Sturdy and thin, with bendable and foldable properties.

• Because of its dense organization and strong covalent connections between atoms, it functions as an effective barrier.

• Very transparent—only 2.3% of the light that passes through it is absorbed.

• The tiniest material ever discovered.

• Inert chemically.

• The fourth pi-electron in graphene prevents a band gap from forming in the conduction band, which makes it extremely conductive to heat and electricity.

• Reasonably priced given the amount of carbon on Earth.

• Adaptable, capable of undergoing a 20% stretch without experiencing any issues.

• Graphene's flexibility pattern can change its magnetic properties, which may make it possible to manipulate its optical, microwave, and conductivity features.

• Graphene displays the quantum Hall effect, in which electrons inhabit quantized energy levels and the Hall conductance assumes quantized values, at low temperatures and strong magnetic fields.

• By doping or other methods, graphene can be made to display semiconducting characteristics, such as a tunable band gap. For instance, doping graphene with

elements like nitrogen or boron can create localized energy levels within the band structure, leading to a semiconducting behavior. This process is known as chemical doping or substitutional doping.

A derivative of graphene with altered physicochemical characteristics, graphene oxide (GO) finds use in particular fields [23].

9. Applications of Gr_PCFs.

Because PCF offers a variety of new or enhanced features that standard fiber cannot, it is finding more and more uses in a wider range of scientific and technological fields [31]. Since two-dimensional (2D) graphene has been discovered, there is currently a lot of interest in merging PCF with graphene. Graphene–PCF (Gr–PCF) combinations have some unique advantages. (1) The atomic thickness of graphene retains the PCF's primary optical capabilities and structure; (2) Its flexibility allows for a tight attachment to the hole walls of the PCF; and (3) Its distinctive features allow for particular functionalities that no other conventional material can match [32].

9.1 Optical Communications

Over the past ten years, PCF technology has developed quickly and shown to be very beneficial for a wide range of intriguing fiber optic communication applications. For high-performance optical networks, the Raman amplification technique has grown in importance. In some applications, it complements erbium doped fiber amplifier (EDFA) technology, while in others, it entirely replaces it [33].

9.1.1 Polarization splitter

Optical devices called polarization splitters, or polarizing beam splitters, or PBSs, divide an incident light beam into two beams having orthogonal polarization states. When exact control over the characteristics of optical signals is needed for a variety of scientific and technical purposes, polarization splitters are crucial in manipulating and controlling polarized light [34].

In 2017, Zou *et al.* [35] a dual-core photonic crystal fiber (PCF) with a graphene layer as the basis was suggested as a polarization splitter. The GD-PCF polarization splitter is a device with a cross-section shown in Fig. 4. It is made up of two cores, A and B, which were formed by solidifying two central

air holes. A layer of graphene, whose thickness is indicated by the symbol t, fills the middle air hole. Four layers of hexagon-shaped air holes with a lattice constant of t make up the device's exterior covering. The backdrop material utilized is pure silica, and the diameter of the air holes is denoted by the symbol d. Pure silica was employed as the background material for the construction. Conversely, the complex refractive index describes graphene.

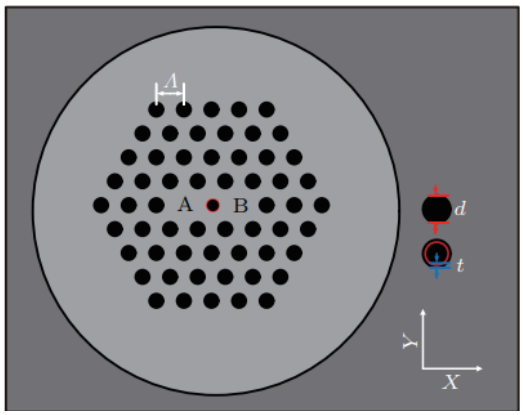

Fig. 4: The cross section of the intended dual-core PCF. The graphene layer is represented by the red annulus, air holes by the black circles, and pure silica by the gray area (online in color) [35].

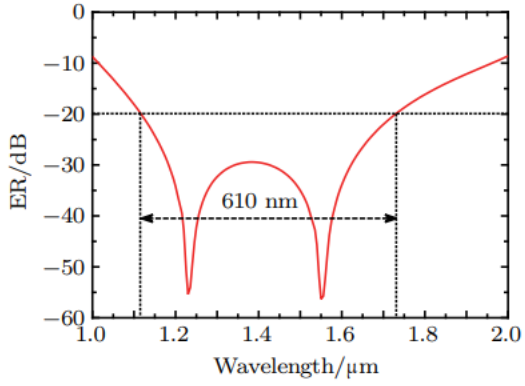

Fig. 5: The optimal values of the extinction ratio are dependent on wavelength (Online color) [35].

The gold standard for evaluating a polarization splitter's performance is the extinction ratio (ER). When the ER is greater than 20 dB, two perpendicular polarization states of light are typically considered to be separated. In the event where incident light enters core A, output port A's ER is defined as:

$$ER = 10\frac{P^{A}_{out,x}}{P^{A}_{out,y}} \qquad (8)$$

In this equation, $P^{A}_{out,x}$ represents the power of the output signal polarized along the x-axis from port A, while $P^{A}_{out,y}$ represents the power of the output signal polarized along the y-axis from port A.

At a wavelength of 1.55 μm, this splitter with a 4.8 mm fiber length achieves an extinction ratio of -56.3 dB according to simulation data. In addition, the splitter exhibits an ultra-broadband width of 610 nm (from 1120 nm to 1730 nm) and an extinction ratio of less than -20 dB, which qualifies it for use in coherent optical communication systems [35].

9.1.2 Modulator

A modulator is a device or circuit that changes the characteristics of a carrier signal in order to transmit information. A modulator is a device or circuit that

changes the characteristics of a carrier signal in order to transmit information. It is used in telecommunications and broadcasting systems to encode data onto a carrier wave, which can then be transmitted over long distances and graphene-based optic modulators have gained attention due to graphene's unique properties. Electro-optic modulators, which can easily be controlled and accessed, are being explored as an alternative to narrow-bandwidth modulators [36].

In 2020, Fu *et al.,* [37] has proposed a Gr-PCF-based small electro-absorption modulator by adding two sizable semicircular holes to the fiber's innermost air holes and covering them with a monolayer of graphene. The modulator improved the interaction between graphene and light. Strong graphene-light interaction was obtained from the optimized structural parameters. The frequency of the incident light is the only factor influencing the modulator's on-off switching point. The suggested modulator performs have a microstructure with five-layer hexagonal concentric rings and comparable air (see Fig. 6). A modification has been made by replacing the innermost six air holes with two semicircular holes. This alteration improves the refractive properties and promotes a more robust interaction between the graphene material and the polarized light.

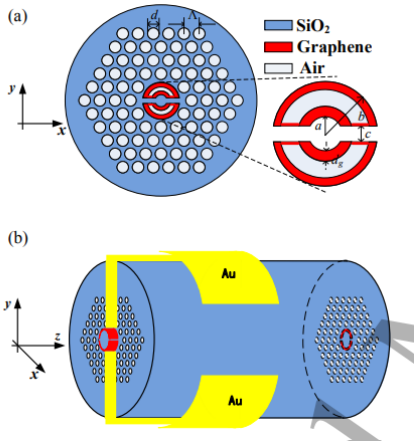

Fig. 6: G-PCF cross-sectional view (a) sectional view (b) in three dimensions [37].

The results showed that on/off switch point of modulator is determined by the frequency of the incident light. By adjusting the physical characteristics of the fiber, the modulator can attain desired qualities including an extinction ratio of 7 dB, a modulation bandwidth of 70 GHz, and a compact footprint of 205 µm. Moreover, the modulator operates in a wide wavelength range, from 1250 nm to 1900 nm [37].

Also in 2020, Xu *et al.,* [38] Attached graphene/hexagonal boron nitride/graphene (Gr/hBN/Gr) films directly to the surface of a photonic crystal fiber (PCF) to create a high-

performance graphene-based optical fiber modulator. This structure can be used to quickly modify the guided light intensity and allowing transmission of single mode over wide bandwidth. The modulated signal has a substantial modulation depth, fast modulation speeds, and low drive voltages. In all-fiber communication systems, this method presents as a good candidate method to incorporate graphene into fiber with good performance. communication systems, this method presents a viable way to incorporate graphene into fiber devices with superior performance.

Similar to Figure 7, the proposed hybrid Photonic Crystal Fiber (PCF) features four circles consisting of air holes with the same diameter and hole pitch surrounding the solid fiber core. By adhering to the hole surface, the Gr/hBN/Gr films form a parallel-plate capacitor structure that is comparable. The electro-optical property of graphene allows the intensity of core-guided light to be adjusted by an external square-wave drive voltage applied in a modest amount. The well-considered proportions of the hole diameter and pitch, in conjunction with the hBN film—which serves as both an optical transparent material and an electrical insulator—ensure single mode transmission throughout all optical communication bands. The combination between unique optical properties of PCF with wide operating wavelength range of graphene and its electrically controllable optical response made Gr-PCF is an excellent option for a broadband fiber modulator [38].

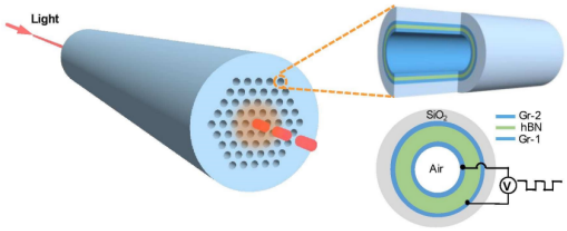

Fig. 7: Diagrammatic representation of a Gr/hBN/Gr PCF modulator sandwiched[38].

The proposed structure given in Fig. 7, allowing the light intensity to be regulated across the fiber by varying a modest external voltage applied to the graphene films. Changing the electric field intensity at the fiber-film interfaces causes change in refractive indices, and allow the interaction between light and grapheme. The transmission attenuation of light through the fiber is dependent on the thickness and number of layers of graphene.

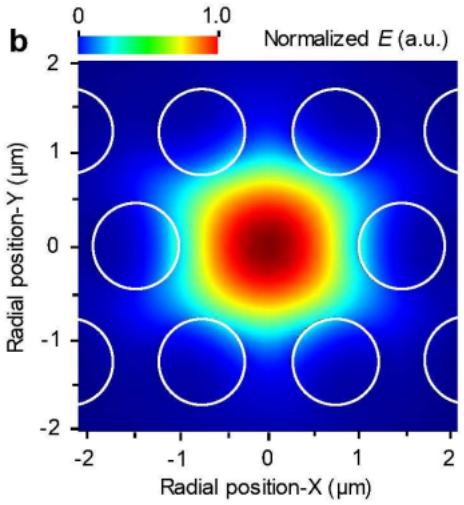

Fig.8: The basic guided mode's electric field distribution in Gr/hBN/Gr PCF was computed using the finite element method. White circles in PCF indicate the boundary of the air hole. Pitch and hole diameter are 1.516 μm and 1 um, respectively. The hole surfaces are covered with two monolayer films of graphene and one monolayer film of hBN[38].

This PCF design serves as the foundation for an in-line modulator that can accomplish single-mode transmission across the whole optical communication band, from 1260 nm to 1700 nm. At 1550 nm, a modulation depth of about 42 dB/mm-1 is attained. It also provides a fast modulation rate of up to 0.1 GHz.Different desired performance indicators can be attained by varying the structural factors, such as fibre length, fibre hole diameter, and the quantity of graphene and hexagonal boron nitride layers [38].

9.1.3 polarization filter

A polarization filter is a device that selectively transmits light of a specific polarization while blocking or attenuating light of other polarizations.

When PCF is filled with metal, there is a noticeable change in the way matter and light interact, especially because surface plasmons, which are collective oscillations of free electrons on the metal's surface, are set off. Through this method, electromagnetic wave energy is coupled to surface plasmons at the resonance frequency and for a specific light polarization.

The way in which light and electron oscillations are connected on a metal surface is referred to as the "surface Plasmon Polariton" (SPP). Surface Plasmon Resonance, or SPR, is the phenomena that this PCF-based ultra-short polarization filter uses. When the core-guided mode aligns with the SPP mode, the filter operates at the resonance frequency, which causes an increase in confinement loss for the core mode [39].

In 2021, Lavanya, A., and G. Geetha. [40] The paper presents a hybrid silver-graphene coated pentagonal photonic crystal fiber (PCF) as the basis for a suggested polarization filter. This filter

successfully blocks the undesired Y-polarized mode with high loss while selectively allowing the required X-polarized mode to flow through with low loss. As illustrated in Fig. 9, the proposed PCF consists of four layers of air holes stacked in a pentagonal lattice configuration, where pitch (Λ) represents the separation between each air hole and diameter (d). With d=1.4 µm, the optimal air filling fraction (d/Λ) for this structure is 0.76. The introduction of silver plating in the air hole of the PCF structure induces surface plasmon resonance (SPR). However, as the distance between the silver-filled air hole and the core region increases, there is a reduction in the strength of the coupling .Consequently, the air hole in the second cladding layer with diameter d1 is selected because it amplifies the near-field interaction .The ideal thickness for the silver coating is_30 nm, whereas the graphene monolayer has a thickness of 0.34 nm.

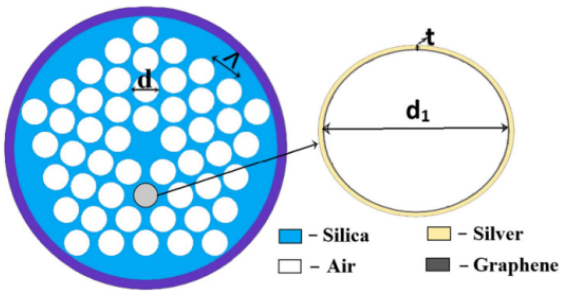

Fig. 9: Diagrammatic cross-section of the PCF-based recommended polarization filter[40].

This hybrid pentagonal lattice PCF-based polarization filter exhibits remarkable performance in terms of polarization separation, cross-talk reduction, minimal confinement loss for desired modes, and broad bandwidth operation. It is coated with both silver and graphene.

At communication wavelengths of 1.31 µm and 1.55 µm, the suggested polarization filter successfully separates the desired X-Polarization mode from the undesired Y-Polarization mode.

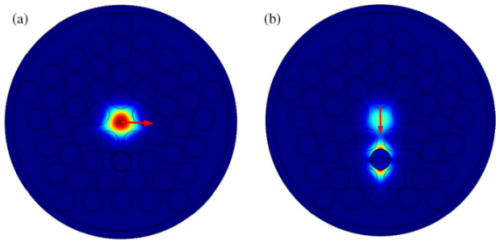

Fig. 10: X- and Y-polarization-related surface plasmon polariton (b) and Feld distribution at 1.55 µm (a)[40].

Low confinement loss for the permitted X-Polarized mode and high confinement loss for the undesirable Y-Polarized mode are the results of the Photonic Crystal Fiber's (PCF) design optimization. The suggested PCF, measuring 300 µm in length, has a wide bandwidth and minimal cross-talk, which makes it appropriate for integrated

optical systems. The suggested PCF's fabrication feasibility is also examined, and the results show that it is feasible to produce.

These findings suggest that the polarizing filter is a good option for integrated optical systems in a variety of applications, such as data transmission networks or communications, due to its superior qualities and small device size [40].

In 2023, Wang, Jianshuai, et al. [41] It was suggested to create a new kind of polarization mode filter that has wavelength switching capabilities. The polarization mode filter's (PMF's) foundation is a D-shaped photonic crystal fiber (PCF) that has been coated in graphene. A coating of gold is added to the top of the PCF to improve the interaction between the fibre and graphene, as seen in Figure 11.

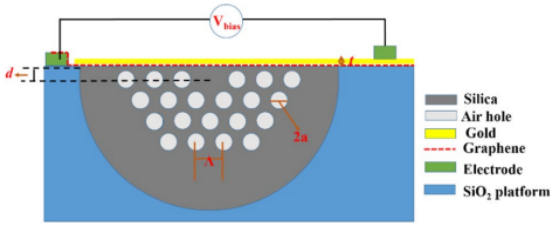

Fig. 11: The suggested adjustable polarization filter's cross section[41].

Extinction ratios are frequently used to quantify a device's ability to suppress undesirable signals. They relate to the filtering capability of the device. The power ratio of the desired signal to the undesirable signal referenced before eq. 9 is expressed [41]

$$ER = 20 * 1g\left(exp\left((a_y - a_x)L\right)\right) \qquad (9)$$

where L is the device length and αx, αy represent the loss of x-pol and y-pol, respectively.

The PMF is intended to filter y-polarized modes by making use of the distinct coupling characteristics between core modes and surface plasmon polariton (SPP) modes. By varying the chemical potential of graphene, the filtering wavelength can be changed to achieve single-, dual-, or triple-wavelength results.

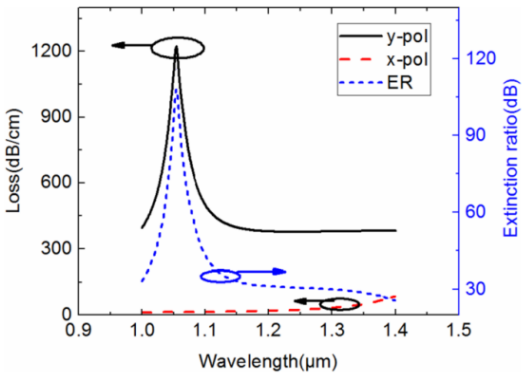

Fig. 12: The parameters of the DAPCF loss at μc=0.3 eV are a=0.85 μm, Ÿ=2 μm, t=40 nm, and d=0.9 μm[41].

The numerical analysis findings demonstrate that, with a tiny device length of only 100 μm, the suggested polarization filter has an extinction ratio

higher than 25 dB over a wavelength range of 1.0 to 1.4 μm. This suggests that the filter is successful in preventing undesirable polarizations from passing through while permitting favourable polarizations to do so. Applications for this technology include multi-parameter sensing, WDM communication systems, and polarization modulation [41].

This work allows for a synopsis of graphene's applications. First off, it strengthens the connection between graphene and fibre, which boosts the polarization mode filter's (PMF) efficiency. The y-polarized modes can be filtered more effectively thanks to this improved interaction. Second, the filtering wavelength can be adjusted by varying the chemical potential (μc) of graphene. This implies that it is feasible to switch between various wavelengths for filtering using a single device. Comparing this wavelength selection freedom to conventional fixed-wavelength filters is a big benefit. Additionally, coating gold on top of graphene further enhances its properties and strengthens its interaction with light waves passing through the fiber. The combination of these materials results in improved performance characteristics such as high extinction ratio (>25 dB) over a wide range (1.0~1.4 μm). Overall, incorporating graphene into this PMF design offers improved functionality and tunability compared to conventional filters without compromising other important parameters like extinction ratio or device length.

9.2 Sensors

Photonic crystal fiber offers a high degree of design flexibility and makes it easier to develop new sensing applications because it allows for variations in the size and location of cladding holes and/or the fiber transmission spectrum's core, dispersion, mode shape, air filling fraction, nonlinearity, and birefringence—all of which can be tuned to reach values that are not possible with conventional optical fibers. In addition, the existence of air holes enables liquids or gases to enter the perforations and light to pass through the atmosphere. This opens up new options for sensing by enabling controlled interaction between light and sample. The photonic crystal fibre applications in the sensing business can be divided into three main categories: chemical, physical, and biosensors,

depending on the characteristic under evaluation [42].

Photonic crystal fibres are used by physical optic sensors to measure physical characteristics such as curvature, temperature, displacement, electric field, magnetic field, refractive index, torsion, and vibration. The measurement, tracking, and control of these attributes are of tremendous relevance to many applications. Physical sensors that measure strain, curvature, torsion, transversal load, and temperature are particularly useful for the purpose of monitoring the structural health. For civil constructions like buildings, bridges, and dams, ongoing monitoring is required in order to regulate and avert aberrant conditions or accidents before they happen [43].

Different physical sensors, including electric and magnetic fields, provide an insulating link to high voltage places that typical electric sensors do not, making them particularly useful for sensing at high voltages [44].

However, surface plasmon resonance (SPR) is a phenomenon that occurs when free electrons collectively vibrate at the interface between a metal and a dielectric material [45].

It is widely used in sensors, where a prism coated in metals, such gold or silver, makes it easier to match the resonant phase between the incident and plasmonic waves. Graphene has lately attracted attention as a potential covering material for surface plasmon resonance (SPR) sensors due to its unique optical conductivity and plasmonic properties. Because of this, graphene is a potential solution for raising the plasmonic device's efficiency [46].

9.2.1 A Refractive Index Sensor

One important basic physical property is the refractive index. Many real-world industries, including food processing, quality control, and liquid adulteration, can benefit from in situ measurement for material identification. Biomolecules can also be identified with it [47].

In 2020, Li, Tianshu, et al. [48] An H-shaped PCF-SPR sensor has been created by researchers to track changes in an analyte's refractive index (RI). Ag-graphene layers are coated in symmetrical U-shaped grooves on the y-axis of the sensor design. Additionally, the asymmetrical design of the sensor provides higher sensitivity to x-polarized light compared to y-polarized light, as depicted in Figure 13.

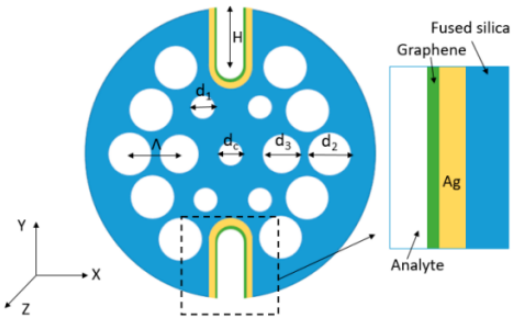

Fig. 13: Diagram showing the Ag-Graphene coated PCF-SPR sensor architecture[48].

Light propagates along the Z axis, and the XY plane is where the modal analysis simulation is carried out. Fused silica is the fiber material utilized, and the Sellmeier equation is used to calculate the material's refractive index (RI):

$$n^2 = 1 + \frac{A_1\lambda^2}{\lambda^2 - B_1} + \frac{A_2\lambda^2}{\lambda^2 - B_2} + \frac{A_3\lambda^2}{\lambda^2 - B_3} \quad (10)$$

where $B_1 = 4.67914826 \times 10{-}3\ \mu m^2$, $B_2 = 1.35120631 \times 10{-}2\ \mu m^2$, and $B_3 = 97.9340025\ \mu m^2$. where $A_1 = 0.696166300$, $A_2 = 0.407942600$, and $A_3 = 0.897479400$._The following formula [11] can be used to determine the RI of graphene:

$$n_g = 3 + \frac{i \times 5.446 \mu m^{-1} \times \lambda}{3} \quad (11)$$

where the vacuum wavelength is denoted by λ. There are L = 12 graphene layers in Figure 1 at tgraphene = 4.08 nm. The thickness of a single layer of graphene is 0.34 nm. The Lorentz-Drude model can be used to calculate the RI of silver.

The suggested sensor offers a broad range of analyte refractive index detection, from 1.33 to 1.41, as shown in Fig. (14). The maximum calculated sensitivity was 12,600 nm/RIU (refractive index unit)_.With a resolution of 3.61 ×10−5 RIU, the average wavelength sensitivity within the linear RI detecting area of 1.33 to 1.36 is found to be roughly 2770 nm/RIU.

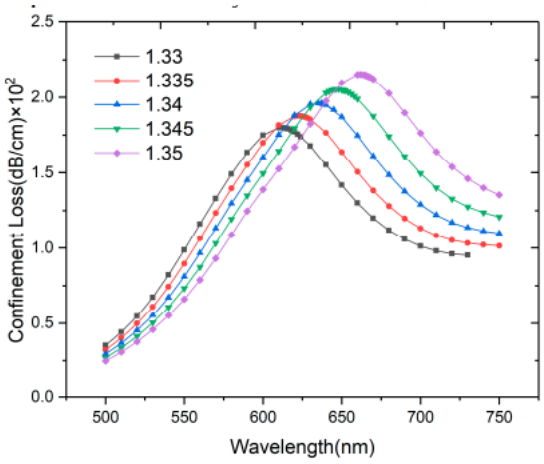

(a)

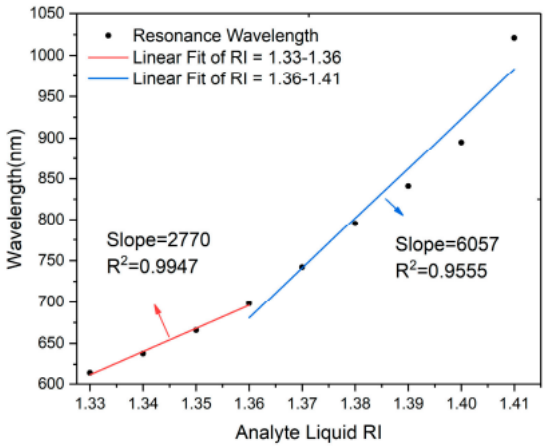

(b)

Fig. 14: (a) The loss spectrum of the developed sensor when na falls between 1.33 and 1.35; (b) The resonance wavelength and relationship

between RI and na when na falls between 1.33 and 1.41[48].

The findings suggest that this study offers significant perspectives for creating sensitive sensors in the future for a range of uses, including biosensing and water pollution monitoring.

In 2021, Faul etal [49] suggested and built a SPR based on PCF. Graphene was used externally to improve the sensing performance of aqueous liquids. The performance of the suggested sensor shows good linear characteristics and high sensitivity for various modes. Figure (15) shows the suggested SPR sensor based on PCF, which consists of three rings of air holes arranged in an octagonal shape around a core diameter of 10 µm. The size and location of air holes were precisely designed to get good coupling energy between propagating modes in PCF and modes that are excited in the graphene layer.

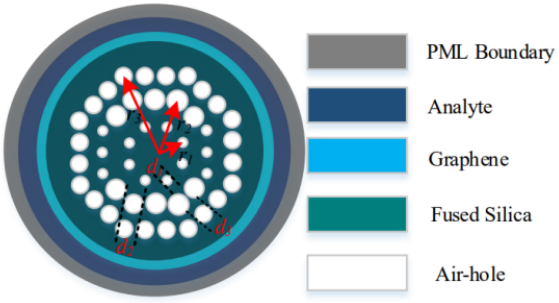

Fig. 15: Diagram illustrating the cross-section of the proposed graphene-coated photonic crystal fiber RI sensor[49].

Phase matching behavior is influenced by the amount of graphene layers, and this in turn affects amplitude sensitivity and confinement loss. The findings indicate that the maximum loss and amplitude sensitivity change with varied analyte refractive indices and polarization modes at a graphene layer thickness of 40.12 nm.

The sensor showed the highest recorded amplitude sensitivities to date: 14,847.03 RIU−1 for the x polarized mode and 7351.82 RIU−1 for the y polarized mode. Furthermore, the sensor demonstrated the ability to detect analyses in aqueous solutions with a figure of merit (FOM) value of 2000 RIU−1 at an analyte refractive index (RI) of 1.332, as well as a resolution value as low as 5.0 × 10−5[49].

In 2023, Xue, Fan, et al .[50] an extremely sensitive plasmatic D-shaped photonic crystal fiber (PCF) sensor with an integrated silver (Ag) grating covered in graphene was presented. As seen in Fig. 16, the graphene layer on the Ag surface aids in slowing down the oxidation process of Ag, improving the sensor's performance.

Notable characteristics of these fibers include their high sensitivity to refractive

index fluctuations and their effective induction of surface Plasmon polarities at the metal-dielectric interface.

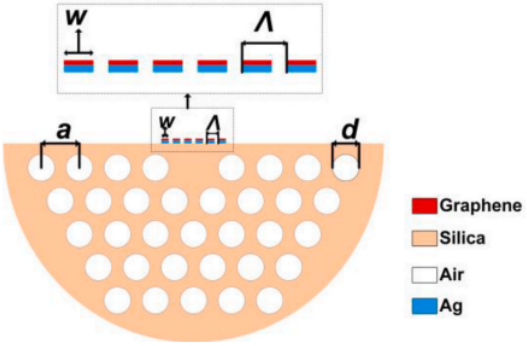

Fig. 16: Shows the D-shaped profile of an aging PCF refractive index sensor [50].

Grating fiber sensors made of pure silica material are less sensitive than other fiber-based sensors; in contrast, optical fiber sensors coated with metal material show comparatively better sensitivity. While they can also reach great sensitivity, D-shaped optical fiber sensors based on metal materials or particular fiber sensors have a smaller range of refractive index (RI) for the intended analytic.

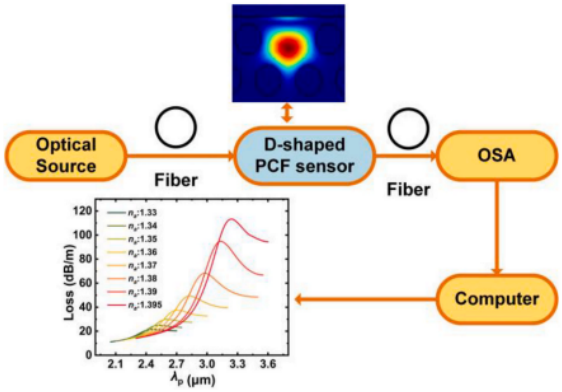

Fig. 17: The suggested plasmonic sensor's basic configuration for measuring refractive index [50].

The sensor reported in the paper has a high resolution of 4.16 × 10^(-6) RIU and an enhanced RI sensitivity of 18612 nm/RIU in the 1.30–1.395 range. The paper also shows how the grating structure and PCF settings affect the loss spectrum, which makes this small sensor useful for a variety of applications like food detection, water quality monitoring, and biomedicine.

9.2.2 A Temperature Sensor

Temperature measurement is a vital parameter in various technological fields, industrial production, maintenance processes, and medical treatments. The advancement of fiber optic sensors has emerged as a valuable alternative to electrical sensors for temperature monitoring, representing a significant breakthrough [47].

In 2019, Paul, Alok Kumar, et al. [51] emphasizes the creation and assessment of a temperature sensor intended for use in electric vehicle (EV) applications. The suggested temperature sensor employs an octagonal photonic crystal fiber (PCF) and blends ethanol as the sensing medium with graphene/gold as a plasmonic material. The two rings of air

holes in the suggested temperature sensor are placed in an octagonal configuration. The air holes in the first and second rings are separated from the core by 0.8 µm, whereas the central air hole has a diameter of 0.1 µm. All air holes have a diameter of 0.15 µm, with the exception of the bigger ones in the second ring. In this sensor design, as shown in fig. (18-a), ethanol, silica, and either graphene or gold are employed as temperature-dependent, background, and plasmonic materials, respectively.

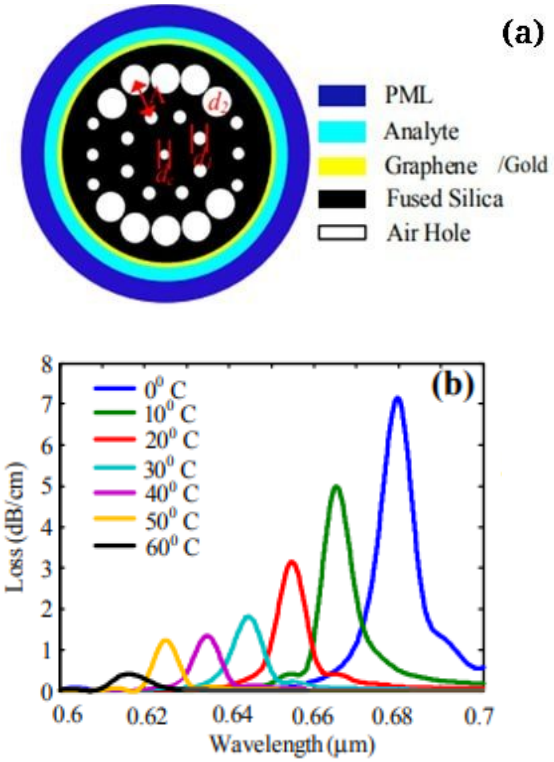

Fig. 18: (a) Temperature sensor based on PCF is proposed ,and (b) loss spectra for various temperatures as a function of wavelength.

From Fig. (18-b), it is clear that , there was a resonance peak for 0°C at a wavelength of 0.6798 µm. Higher temperatures were represented by successive peaks that occurred at different wavelengths. In the case of gold plasmonics, a resonance peak was seen at 0.6653 µm at 10°C, and its wavelength varied as the temperature rose.

The temperature/wavelength sensitivity is computed as follows using the wavelength interrogation method.

$$S = \frac{\Delta\lambda_{peak}}{\Delta T}\ [nm/°C] \qquad (12)$$

where the resonant peak shift (Δλpeak) and temperature change (ΔT) are presented, respectively.

The maximum sensitivity achieved was found to be approximately 1450 pm/°C with graphene plasmonic material and 2500 pm/°C with gold plamonic material when calculated through the wavelength interrogation method [51].

In 2021, Cheng, Xu, et al. [52] developed a highly sensitive and versatile temperature sensor known as the graphene photonic crystal fiber (Gr-PCF) sensor. This innovative sensor overcomes the limitations of previous transfer-based graphene sensors, which had low sensitivity and distorted transmission characteristics. The

proposed hybrid design maintains the structural integrity and transmission mode of the fiber while greatly enhancing the temperature detection capability of graphene by embedding it into the holes of the photonic crystal fiber (PCF).

As shown in fig. 19, the PCF is made up of six sporadically placed air holes in the cladding, each with a diameter (Φ) of 2.22 μm and a pitch (Λ) of 5.4 μm.

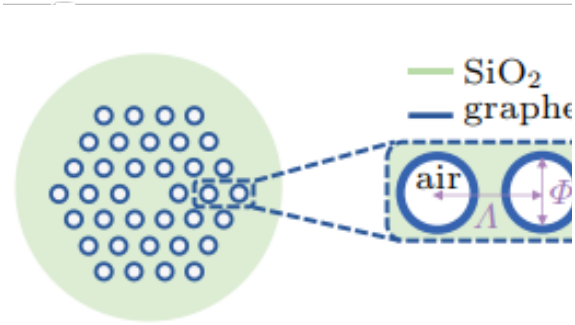

Fig. 19: shows the full covering of graphene sheet on the inner surface of the PCF cladding air holes (the hole width Φ and pitch Λ are both micron-scale). Gr-PCF cross-section diagram[52].

Through simulations, it is found that the temperature sensitivity may be set four orders of magnitude up to around 3.34 × 10-3 dB/(cm•◦C) when the graphene Fermi level is about 35 meV higher than half the input photon energy.Moreover, the sensitivity can be increased by around ten times by improving the PCF structure, such as the fiber hole diameter, which would improve the light-matter interaction. These results provide a new way to develop ultra-sensitive temperature sensors and increase the range of applications of these sensors in all-fiber optoelectronic devices [52].

9.2.3 Humidity sensor

A device employed to measure the moisture or water vapor content in the atmosphere. It detects changes in humidity and converts them into an electrical signal, which can be employed for monitoring and controlling the environment [53].

In 2020, Li, Jia-xin, et al. [54] created a temperature and humidity sensor with a graphene oxide (GO)-coated photonic crystal fiber (PCF). The sensor works on the basis of the Mach-Zehnder interferometer principle, which states that variations in humidity and temperature have an impact on the interference spectrum. With differences in humidity, a GO layer with hydrophilic characteristics is deposited onto the PCF surface, causing notable changes in refractive index. High sensitivity to temperature and humidity is demonstrated in experimental results, which makes this sensor a desirable choice for a range of applications. It also

has benefits like inexpensive cost and easy construction. Two types of fiber were used in this study: single-mode fiber (SMF-28) and photonic crystal fiber (PCF). The PCF measured 125 µm in outer diameter, 10.1 µm in core diameter, 2.85 µm in hole diameter, and 7 µm in hole pitch. As shown in fig. 20, the SMF-28 had a core diameter of 8.2 µm and a cladding diameter of 125 µ m.

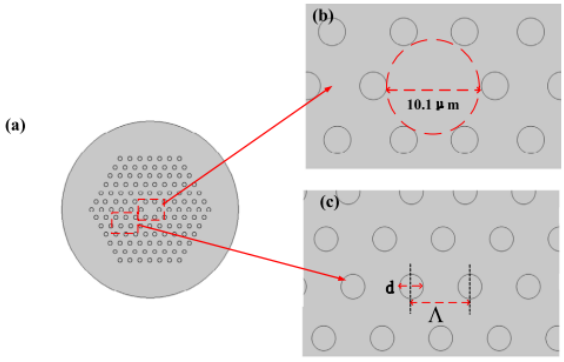

Fig. 20: (a) The LMA-10-PCF cross-section schematic. (b) The LMA-10-PCF's core diameter. (c) an in-depth LMA-10-PCF cross-section[54].

The temperature sensitivities of the sensor are 0.063 nm/°C and 0.086 nm/°C within a temperature range of 10°C to 70°C, respectively, according to the numerical simulation results in this study. The sensor's humidity sensitivities are determined to be 0.159 nm/%RH and 0.128 nm/%RH, respectively, throughout a humidity range of 30% to 70%[54].

9.2.4 Magnetic field sensor

A magnetic field sensor is a device that measures the direction and strength of a magnetic field. It can detect changes in the magnetic field and convert them into an electrical signal for use or further research.

In 2020 Liu, Hai, et al. [55] provided a suggested technique for utilizing Surface Plasmon Resonance (SPR) in a twin-core photonic crystal fiber (PCF) to measure temperature and magnetic field simultaneously. Through loss-peak changes in the output spectra and the deposition of a silver-graphene layer and the infiltration of magnetic fluid (MF), the authors manipulate the twin-core structure to achieve simultaneous measurement. Furthermore, they ensure that light propagation in the two cores does not interact by improving temperature sensitivity and allowing the construction of two distinct sensing mechanisms by filling the cladding air holes with a mixture of toluene and chloroform.

To accomplish the requisite sensing capabilities, as shown in fig. 21, the sensor makes use of a twin-core photonic crystal fiber (PCF) with certain hole sizes and a center hole covered with a

silver-graphene layer and filled with a specific material (MF).

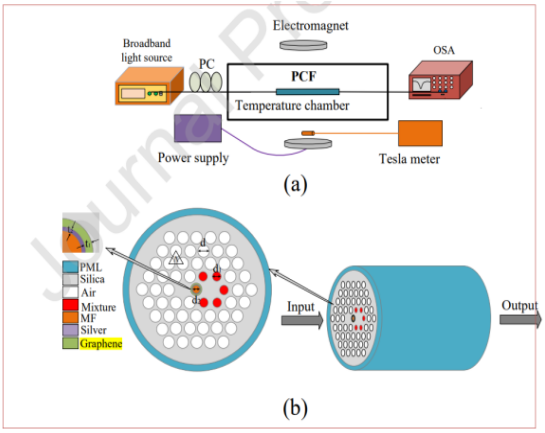

Fig. 21: Shows the fundamental diagram for the PCF cross-section and the demodulation technique[55].

connection between temperature and peak shifts.

$$[\Delta\lambda_1\ \Delta\lambda_2\ ] = [K_1\ K_2\ K_3\ K_4\ ][\Delta B\ \Delta T\ ] \quad (13)$$

$$[\Delta B\ \Delta T\ ] = [K_1\ K_2\ K_3\ K_4\ ]^{-1}[\Delta\lambda_1\ \Delta\lambda_2\ ] \quad (14)$$

By detecting shifts in the output spectra, the authors are able to perform the simultaneous measurement. Due to the high sensitivity in temperature (0.37nm/°C) and magnetic field (0.44nm/mT) provided by the proposed dual-parameter demodulation approach, this dual-core PCF structure can measure a variety of environmental factors [55].

In 2021 Xiao, Gongli, *et al.* [56] focused on creating a multi-parameter integrated detecting sensor with surface plasmon resonance (SPR) and photonic crystal fiber (PCF). The temperature, magnetic field, and refractive index can all be detected by the sensor. The sensor measures these parameters precisely by applying a gold film to the PCF's air holes, adding magnetic fluid, and using a temperature-sensitive substance. To improve sensitivity, a graphene layer is also applied. Simulation results show that this sensor works effectively for measuring temperature and magnetic field intensity within their respective ranges, and for detecting refractive index within a specified range.

The optical fiber is made up of four layers with 19 air holes placed in a parallel configuration. The initial layer of the layout has a horizontal line of air holes with two on each side. The goal of adding these air holes is to form a solid photonic crystal fiber, which improves nonlinear effects and increases field strength by improving light confinement in the fiber core. The temperature-sensitive medium (PDMS) and magnetic fluid (MF), respectively, are inserted into the air pores on either side of the fiber core that have been coated with a gold coating. Figure 22 illustrates the addition of a graphene layer to the gold film in order to increase sensitivity.

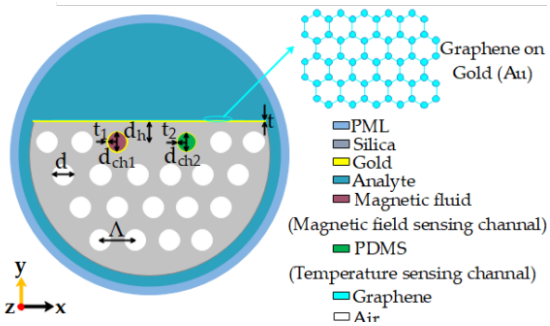

Fig. 22: Schematic illustration of the two-dimensional cross-section structure of a plasmonic optical fiber sensor [56].

By figuring out channels 1 and 2's resonant wavelength offsets, integrated temperature and magnetic field sensing can also be accomplished. The wavelength measurement method's sensitivity calculation algorithm is as follows.

$$K_{ch}(T) = \frac{\Delta\lambda_{ch}}{\Delta T} \qquad (15)$$

$$K_{ch}(H) = \frac{\Delta\lambda_{ch}}{\Delta H} \qquad (16)$$

The following is the expression for the sensing matrix that is used to determine the temperature and magnetic field change:

$$(\Delta T\ \Delta H\ ) = (K_{ch1}(T)\ K_{ch1}(H)\ K_{ch2}(T)\ K_{ch1}(H)\ )^{-1}(\Delta\lambda_1\ \Delta\lambda_2\ ) \qquad (17)$$

An equation can be used to calculate the change in temperature and magnetic field by sensing the offset of the resonant wavelength and obtaining the simultaneous detection of temperature and magnetic field (17).

The outcomes of the simulation are displayed.First, refractive index detection: The planned refractive index channel has an average sensitivity of 17,571 nm/RIU and a maximum sensitivity of 76,000 nm/RIU.Second, the sensor's sensitivity to magnetic field intensity is evaluated at 164.06 pm/Oe for magnetic field intensity detection. Finally, the temperature sensitivity of the sensor is evaluated at -5001.31 pm/°C for temperature detection [56].

10. Conclusions

The combination of photonic crystal fibres (PCFs) with graphene offers a number of significant advantages, such as broadband optical qualities, robust light-matter interaction, optical properties that may be tuned, ultrafast response times, strong light absorption, and plasmonic effects. Because of these characteristics, graphene is a very promising material for improving PCF functionality and performance, opening up a variety of applications in fields like nonlinear optics, optoelectronics, sensing, telecommunications, Optical modulators, photodetectors, optical switches, nonlinear optics, biosensors, fiber lasers, and quantum optic.

When integrating graphene with PCFs, there are, nevertheless, some restrictions and problems to take into account that include the difficulty of fabrication, the atomically thin nature of graphene and its relatively short interaction length with light, the sensitivity of graphene to temperature, humidity, and chemical exposure in the environment, and the difficulties of producing high-quality graphene on a large scale for PCF integration.

In this review paper, a general introduction is provided about photonic crystal fiber and graphene, highlighting the characteristics of each. The emergence of graphene has opened up new opportunities when combined with PCFs, allowing for electrical tunability, a broadband optical response, and all-fiber integration ability. The review also covers the applications of plasmonic photonic crystal fibers, including in optic communications and various physical sensors.

References

[1] Falah, F.H., ,2019, An overview of photonic crystal fiber (PCF). Indian Journal of Natural Sciences, 9 (5), 30976-0997.

[2] Philip, R, 2003, 2004, Photonic crystal fibers, science, 299, 5605, 358-362.

[3] Buczynski, R. J, Photonic crystal fibers, Acta Physica Polonica A 106 (2), 141-167.

[4] Russell, P., 2003, Photonic-crystal fibers, Science, 299, 358–362.

[5] Zolla, F., Renversez, G., Nicolet, A., Kuhlmey, B., Guenneau, S., Felbacq, D., 2005, Foundations of Photonic Crystal Fibers, Imperial Collage Press, London.

[6] Shefali, S., and Singal, P., 2017, Photonic crystal fiber: construction, properties, developments and applications. Int. J. Electron. Eng 9, 1-8.

[7] Juan, H.D.J., Xu, Z., and Ping, P. 2019, Review on photonic crystal fibers with hybrid guiding mechanisms. IEEE Access 7, 67469-67482.

[8] Zolla, Frédéric, 2005, Foundations of photonic crystal fibres. World Scientific.

[9] Pinto, Ana MR, and Manuel Lopez-Amo, 2013, All-fiber lasers through photonic crystal fibers. Nanophotonics, 2 (5-6), 355-368.

[10] Tuomo, R., 2006, Novel sensor and telecommunication applications of photonic crystal fibers. Helsinki University of Technology.

[11] Chen, M., Yu, R., and Zhao, A., 2005, IEEE Confinement Losses and

Optimization in Rectangular-Lattice Photonic-Crystal Fibers, Journal of light wave technology, 23, (9).

[12] Xiao, L., Demokan, M. S., Wang, Y., and Zhao, C., 2007, Fusion Splicing Photonic Crystal Fibers and Conventional Single-ModeFibers:Microhole Collapse Effect. Journal of Lightwave Technology, 25.

[13] Yang, K., Chau, Y., Huang, Y., Yeh, and Tsai, D.P., 2011, Design of high birefringence and Low Confinement Loss PhotonicCrystal Fibers with five rings hexagonal and octagonal symmetry air-holes in fiber cladding, Journal of Applied Physics.

[14] Johny, J., 2012, Determination of Photonic Crystal Fiber Parameters with effects of Nonlinearities in Supercontinuum Generation, Optical Networking Technologies and Data Securities (OPNTDS).

[15] Abdul, R., Photonic Crystal Fiber.

[16] Lou, J., Surface plasmon resonance photonic crystal fiber biosensor based on gold-graphene layers. Optical Fiber Technology 50, 2019, 206-211.

[17] Susobhan, D., Haldar, R., and Varshney, S. K., 2013, Triple-core collinear and noncollinear plasmonic photonic crystal fiber couplers. Applied Optics 52 (34), 8199-8204.

[18] Homola, J., 2008, Surface plasmon resonance sensors for detection of chemical and biological species. Chem. Rev. 108, 462–493.

[19] Fu, H.Y., Zhang, S.W., Chen, H., Weng, J., 2015, Graphene enhances the sensitivity of fiber-optic surface plasmon resonance biosensor. IEEE Sens. J. 15, 5478–5482.

[20] Luan, N., Yao, J.: 2017, A hollow-core photonic crystal fiber-based SPR sensor with large detection range. IEEE Photon J. 9, 1–7.

[21] Tiwari, S.K., Kumar, V., Huczko, A., Oraon, R., Adhikari, A.D., Nayak, G., 2016, Magical allotropes of carbon: prospects and applications. Crit. Rev. Solid State Mater. Sci. 41(4), 257–317

[22] Yang, Y., Liu, R., Wu, J., Jiang, X., Cao, P., Hu, X., Pan, T., Qiu, C., Yang, J., Song, Y., Wu, D., Su, Y., 2015, Bottom-up fabrication of graphene on silicon/silica substrate via a facile soft-hard template approach. Sci. Rep. 5, 13480.

[23] Patel, Shobhit K., 2023, Recent Advances in Graphene Nanophotonics. Springer.

[24] Katsnelson, M.I., 2007, Graphene: carbon in two dimensions. Mater. Today 10, 20–27.

[25] Lagendijk, A., Tiggelen, B.V., Wiersma, D.S. 2009, Fifty years of Anderson localization. Phys. Today 62, 2429.

[26] Geim, A.K., Grigorieva, I.V., Der, V., 2013, Waals heterostructures. Nature, 499, 419–425.

[27] Xu, Z., Buehler, M.J., 2010, Geometry controls conformation of graphene sheets: membranes, ribbons, and scrolls. ACS Nano 4, 386–387.

[28] Park, S., Ruoff, R.S., 2009, Chemical methods for the production of graphenes. Nat. Nanotechnol. 4, 217–224.

[29] Nair, R.R., Blake, P., Grigorenko, A.N., Novoselov, K.S., Booth, T.J., Stauber, T., Peres, N.M.R., Geim, A.K., 2008, Fine structure constant defines visual transparency of graphene. Science 320, 1308.

[30] Kelly, B.T., 1981, Physics of Graphite. Applied Science Publishers, London.

[31] Philip, R., 2003, Photonic crystal fibers, science, 299 (5605), 358-362.

[32] Chen, K., 2019, Graphene photonic crystal fibre with strong and tunable light–matter interaction, Nature, Photonics, 13(11), 754-759.

[33]. Hasan, D. M. N., Hossain, M. N., Mohsin, K. M., 2011, Analysis of Micro and Nanostructured Photonic Crystal Fibers, Doctoral dissertation, Bangladesh University of Engineering and Technology.

[34] Lin, Z., 2005, PCF-based polarization splitters with simplified structures, Journal of lightwave technology 23 (11), 3558.

[35] Hui, Z,, 2017, Ultra-broadband polarization splitter based on graphene layer-filled dual-core photonic crystal fiber, Chinese Physics B, 26 (12), 124216.

[36] Zhi-Bo, L., 2013, Broadband all-optical modulation using a graphene-covered-microfiber. Laser Physics Letters 10 (6), 065901.

[37] Guangwei, F., 2020, A compact electro-absorption modulator based on graphene photonic crystal fiber, Chinese Physics B 29 (3), 034209.

[38] Xu, C., 2020, Sandwiched graphene/hBN/graphene photonic crystal fibers with high electro-optical modulation depth and speed, Nanoscale 12(27), 14472-14478.

[39] Burstein, E., Surface polaritons—propagating electromagnetic modes at

interfaces, Journal of Vacuum Science and Technology 11(6), 1974, 1004-1019.

[40] Lavanya, A., and G. Geetha, 2021,Broadband polarization filter based on hybrid silver-graphene coated pentagonal photonic crystal fiber, Optical and Quantum Electronics 53, 1-15.

[41] Jianshuai, W., Wavelength-Switchable Polarization Filter Based on Graphene-Coated D-Shaped Photonic Crystal Fiber, Plasmonics, 2023, 1-8.

[42] Pinto, A. M. and Lopez-Amo, M., 2012, Photonic crystal fibers for sensing applications, Journal of Sensors, 2012.

[43] López-Higuera, J. M., Cobo, L., A. Incera, Q., and Cobo, L. R., 2011, Fiber optic sensors in structural health monitoring, Lightwave Technology, Journal of, 29, 587-608.

[44] Culshaw, B., 2000, Fiber optics in sensing and measurement, Selected Topics in Quantum Electronics, IEEE Journal of, 6, 1014-1021.

[45] Kretchmann, E., and Raether, Z. H., 1968, Radiative decay of non-radiative surface plasmons excited by light, Z. Naturforsch. A, Phys. Sci., 23, 2135–2136,

[46] Choi, S. H., 2011, Graphene on silver substrates for sensitive surface plasmon resonance imaging biosensors, Opt. Express, 19 (2), 458–466.

[47] Moutusi, D., Gangopadhyay, T. K., and Singh, V.K., 2019, Prospects of photonic crystal fiber as physical sensor: An overview, Sensors 19(3), 464.

[48] Tianshu, L., 2020, A refractive index sensor based on H-shaped photonic crystal fibers coated with Ag-graphene layers. Sensors, 20(3), 741.

[49] Kumar, P.A., 2021, Graphene-coated highly sensitive photonic crystal fiber surface plasmon resonance sensor for aqueous solution: Design and numerical analysis, Photonics. 8(5).

[50] Fan, X., 2023, Ultra-high sensitive refractive index sensor based on D-shaped photonic crystal fiber with graphene-coated Ag-grating, Heliyon 9(4).

[51] Kumar, P.A., 2019, Graphene/gold based photonic crystal fiber plasmonic temperature sensor for electric vehicle applications, 22nd International Conference on Electrical Machines and Systems (ICEMS), IEEE.

[52] Xu, C., 2021, Tunable and highly sensitive temperature sensor based on graphene photonic crystal fiber, Chinese Physics B 30(11), 118103.

[53] Li, T., Dong, X., Chan, C. C., Ni, K., Zhang, S., and Shum, P.P., 2013, Humidity sensor with a PVA-coated

photonic crystal fiber interferometer. IEEE Sensors Journal 13(6), 2214-2216.

[54] Jia-xin Li, Zheng-rong Tong, Lei Jing, Wei-hua Zhang, Juan Qin, Jing-wei Liu, 2020, Fiber temperature and humidity sensor based on photonic crystal fiber coated with graphene oxide, Optics Communications, 467, 125707.

[55] Hai, L., Chen, C., Wang, H., Zhang, W., 2020, Simultaneous measurement of magnetic field and temperature based on surface plasmon resonance in twin-core photonic crystal fiber. Optik, 203, 164007.

[56] Xiao, G., Ou, Z., Yang, H., Xu, Y., Chen, J., Li, H., Li, Q., Zeng, L., Den, Y., Li, J., 2021, An integrated detection based on a multi-parameter plasmonic optical fiber sensor, Sensors, 21(3), 803.